Using Modern Coexistence Theory to understand community disassembly

Joe Brennan[1,2,*]

Sebastian J. Schreiber[1,2]

1. Department of Evolution and Ecology, University of California, Davis USA 95616;

2. Center for Population Biology, University of California, Davis USA 95616;

∗ Corresponding author; e-mail: jlbrennan@ucdavis.edu.

Keywords: community disassembly, secondary extinction, modern coexistence theory, extinction, coexistence

Abstract

Community disassembly considers how the loss of one species affects the dynamics of an ecological community. In some cases, the extinction of a single species can trigger the loss of others, known as secondary extinctions. These secondary extinctions often result from complex species interactions, making it difficult to identify the underlying mechanisms. Here, we leverage Modern Coexistence Theory to identify when and why secondary extinctions occur during community disassembly. To understand when secondary extinctions occur, we develop the Community Disassembly Graph, describing transitions between coexisting communities due to extinction through an invasion growth rate approach. Once a secondary extinction is identified on the Community Disassembly Graph, we decompose the invasion growth rates associated with the secondary extinction to understand why it occurs. We demonstrate the utility of this framework by applying it to models in which different species interactions – competition, facilitation, and predation – significantly contribute to coexistence, with their loss inducing secondary extinctions. Our results show that Modern Coexistence Theory offers a flexible and interpretable approach to understanding when and why secondary extinctions occur in ecological models.

1 Introduction

Species participate in a complex, entangled web of interactions. These interactions can result in the persistence of one species depending on the persistence of another species in the community (Paine, 1966; Lubchenco, 1978; Ebenman and Jonsson, 2005; Jordán, 2009; Langendorf et al., 2025). Consequently, the loss of this species causes the extinction of the dependent species, known as a secondary extinction (Brodie et al., 2014). Secondary extinctions are speculated to contribute significantly to the loss of diversity globally under anthropogenic change across a wide variety of taxa (Moir et al., 2010; Colwell et al., 2012; Strona and Bradshaw, 2018; Kehoe et al., 2021).

When there is a strong, direct dependency of one species on another species, the cause of secondary extinction is often clear. This is the case for predators that rely on their prey or obligate mutualists that depend on their partners. Most theoretical studies investigating the impacts of extinction on communities, known as community disassembly (Ostfeld and LoGiudice, 2003; Zavaleta et al., 2009), focus on these direct types of contingent coexistence. A common approach to identify secondary extinctions uses static food webs or mutualist networks where interactions between species are modeled, but changes in species densities are ignored. To study disassembly in these models, practitioners remove a node corresponding to a species and all associated edges corresponding to some species interaction (predation and obligate mutualism respectively) and declare that species with no more resources or mutualists experience secondary extinction (Dunne et al., 2002b; Memmott et al., 2004; Bane et al., 2018). These studies have provided important insights into how the structure of ecological networks impact the community disassembly process (Dunne et al., 2002b, 2004; Bascompte and Stouffer, 2009; Tang et al., 2024).

Although these studies provide a level of tractability that is difficult to achieve in dynamic models, they neglect well-established mechanisms of secondary extinction that arise from indirect effects. For example, Paine (1966) studied changes in diversity of a rocky intertidal community following removal of the top predator *Pisaster ochraceus*. This loss of predation led to unregulated growth of the prey species *Mytilus californianus* and *Mitella polymerus*, ultimately leading to the secondary extinction of six other species. These secondary extinc-

tions would not be predicted by the static approach as *P. ochraceus* was neither a mutualist nor resource. Only by studying the strength of the interactions and associated dynamics of the community can one understand what led to the dramatic reduction in diversity following loss of the keystone predator *P. ochraceus* (Paine, 1980; Paine et al., 2010). Secondary extinctions have been attributed to the loss of other indirect mechanisms such as ecosystem engineering (Wright et al., 2002; Yeakel et al., 2020) and intransitive competition (Jackson and Buss, 1975; Kerr et al., 2002; Edwards and Schreiber, 2010). The exclusion of these mechanisms of secondary extinction biases our understanding of community disassembly and leads to underestimates of secondary extinctions. By incorporating both direct and indirect mechanisms into community disassembly studies, we can more accurately predict the susceptibility of ecological communities to secondary extinctions.

However, identifying the main drivers of secondary extinctions can be complicated by the cumulative impact of multiple ecological drivers and interactions among these factors (Colwell et al., 2012; Brodie et al., 2014). A secondary extinction might occur only when all remaining species collectively exert competitive pressure, or it might result from a single, competitively dominant species. For example, in systems with a single limiting resource that is supplied at a constant rate, one species alone can be sufficient to exclude others (Gause, 1934; Tilman, 1982). In contrast, microbial communities with tradeoffs in lag and growth rates can allow all pairs of species to coexist but not the full community (Manhart and Shakhnovich, 2018), implying that multiple competitors are needed for exclusion of a single species. In such cases of emergent exclusion, disentangling the relative importance of ecological mechanisms is required to understand what specific mechanisms drive secondary extinctions.

Modern Coexistence Theory (MCT) is an increasingly popular framework that quantifies how multiple, interacting ecological mechanisms influence coexistence outcomes. MCT's key metric is the invasion growth rate (IGR), defined as the per capita growth rate of an invading species when at low density while other species are at some coexistence state. MCT decomposes this IGR to identify what mechanisms promote the successful invasion of the species (Chesson, 1994; Barabás et al., 2018; Ellner et al., 2019). However, these same techniques can also explain what mechanisms most strongly impede successful coexistence or result in

invasion failure (Grainger et al., 2019a; Shoemaker et al., 2020; Spaak and Schreiber, 2023). Therefore, we can leverage MCT to quantify the mechanisms that enable persistence of the secondarily extinct species in the full community with the keystone species, but lead to their exclusion in the post-extinction community. Here, we identify when and why secondary extinctions occur using techniques from MCT. To identify when secondary extinctions occur, we develop the Community Disassembly Graph, detailing how the extinction of a species alters community composition. To understand then how a secondary extinction occurs, we use invasion growth rate decompositions from MCT to understand what ecological drivers led to the secondary extinction.

2 Methods

2.1 Defining the Community Disassembly Graph

To model the dynamics of ecological communities, we use deterministic differential and difference equations where $x_i(t)$ denotes the species density at time t. The differential equations take the form $\frac{dx_i}{dt} = x_i f_i(x)$ where $f_i(x)$ is the per-capita growth rate of species i at community state $x = (x_1, x_2, \ldots, x_n)$. The discrete-time models take the form $x_i(t+1) = x_i(t)F_i(x(t))$ where $F_i(x)$ is the per-capita fitness at community state x. For the discrete-time models, $f_i(x) = \ln F_i(x)$ corresponds to the per-capita growth rate of species i. For these models, there are various ways to define coexistence (Schreiber, 2006; Clark et al., 2024). Here, we define coexistence as a feasible attractor (Clark et al., 2024). Namely, there exists a steady state (or more generally invariant set) at which all the species densities are positive and the species return to this steady state following sufficiently small perturbations of the species densities. Similarly, for any subset of species, coexistence occurs if the model restricted to those species has a feasible attractor.

When a set of species in a community coexist, the extinction of a species, say species i, typically will lead to the community dynamics settling to a new feasible attractor (coexistence state) for the system without species i. These coexistence states are known as a $-i$ communities (Chesson, 1994; Hofbauer and Schreiber, 2022). For a given set of coexisting species,

we can identify the $-i$ community for each species in the community. If all coexisting communities are known, we can find all $-i$ communities for each community. With this, we can identify all possible transitions between coexisting communities due to extinction of a species. To visualize this, we define the Community Disassembly Graph. The nodes of the Community Disassembly Graph are coexisting communities while directed edges are transitions between coexisting communities due to extinction of some species i; precisely, the directed edge goes from the pre-extinction community to the $-i$ community for a given species i. Using the Community Disassembly Graph, we can identify whether a secondary extinction occurs by checking if a $-i$ community has two or more less species than the pre-extinction community.

2.2 Using IGRs to identify $-i$ communities and secondary extinctions

We can solve for $-i$ communities using IGRs, defined as the per-capita growth rate of a species when rare and resident species are at stationarity (Hofbauer and Schreiber, 2022). For differential equations, the IGR of species i at some coexistence state is defined as

$$\lim_{T\to\infty} \frac{1}{T} \int_{t=0}^{T} f_i(x(t))dt$$

while for difference equations, they are defined as

$$\lim_{T\to\infty} \frac{1}{T} \sum_{t=0}^{T} \ln F_i(x(t))$$

IGRs are typically used to identify if a species can successfully invade a coexisting community. If the IGR of a species is positive, the invading species can successfully invade the community, typically leading to some change in community composition (see, however, Mylius et al. (1998) and Mylius and Diekmann (2001) for the resident strikes back phenomenon). If the IGR of a species is negative, upon introduction into the community, its species abundance will decay to extinction.

Let $S \subseteq \{1, 2, \ldots, n\}$ be a subset of coexisting species. A community T is a $-i$ community of community S if $T \subseteq S\backslash\{i\}$ and all species present in community S but not in community T disregarding species i – that is, $T\backslash(S\backslash\{i\})$ – have a negative IGR at community T (Ches-

son, 1994; Ebenman and Jonsson, 2005; Hofbauer and Schreiber, 2022). The latter condition allows us to identify species that experience secondary extinction: species in the pre-extinction community disregarding species i that have a negative IGR at the $-i$ community experience a secondary extinction following the loss of species i. If the loss of species i induces the secondary extinction of other species, we consider species i to be a keystone species (Paine, 1969).

2.3 Decomposing invasion growth rates to determine the causes of secondary extinction

Having identified a secondary extinction event from the Community Disassembly Graph, we want to understand the relative importance of ecological factors underlying this event. To identify their relative importance, we apply the MCT approach to the two IGRs associated with the secondary extinction event. Say species j went extinct following the loss of species i. We know that species j then has a negative IGR at the $-i$ community. To understand why species j has a negative IGR at the $-i$ community, we can decompose its IGR to quantify what aspects of the system impede its establishment. There exist several ways to decompose IGRs (Chesson, 1994; Ellner et al., 2019). Here, we use the method proposed by Ellner et al. (2019) because of its flexibility and broad applicability. The method assesses how different ecological factors impact the IGR of the invading species relative to the resident species. If one of these factors is comparatively more beneficial (or less harmful) to the invading species than the resident competitors, this factor positively contributes to the IGR of the invading species. If the attribute is comparatively more beneficial (or less harmful) to the resident competitors than the invading species, it contributes negatively to the IGR of the invading species (Ellner et al., 2019). Identifying the relative contributions of ecological factors resulting in species j's IGR being negative identifies the relative importance of these ecological factors in preventing species j from establishing in the $-i$ community.

Although this identifies why species j cannot persist following the loss of species i, it does not explain how species i promotes persistence of species j. Thus, we also identify the $-j$ community and decompose the IGR of species j at the $-j$ community. If the persistence of

species i does not depend on the presence of species j (e.g., obligate mutualism), we expect species i to be in the $-j$ community. Furthermore, if the pre-extinction community coexists under the permanence criterion, then species j will have a positive IGR at the $-j$ community (Hofbauer and Schreiber, 2022). By decomposing the IGR of species j at the $-j$ community, we can understand what attributes of the system in the $-j$ community that are not in the $-i$ community allow species j to invade successfully.

We employ this framework on three different models, each in which different species interactions help maintain coexistence of the full system: competition, facilitation, and predation. In each of these cases, the species interaction contributes significantly to the persistence of the full community and thus, following loss of the species mediating this interaction, another species experiences extinction. By using the framework on three examples, we demonstrate the flexibility and utility of our approach.

3 Applications

3.1 Competition

Historically, competition has been viewed as a species interaction that prevents species from coexisting within a community (Armstrong and McGehee, 1980; Pastore et al., 2021). However, competition can also promote coexistence by suppressing the densities of competitively dominant species, allowing otherwise inferior competitors to persist (Edwards and Schreiber, 2010; Levine et al., 2017). To illustrate this type of indirect facilitation, we analyze an empirically parameterized model of a competitive annual plant community (Van Dyke et al., 2022).

Van Dyke et al. (2022) examined how coexistence outcomes change under different precipitation regimes. The model tracks annual seed production. The seeds germinate with some probability g_i or go into the seed bank. If seeds enter the seed bank, they survive with probability s_i to the next year. For seeds that germinate, they produce seeds that then must compete with other seeds before reproducing the following year. Under these assumptions, Van Dyke et al. (2022) describe the model as

$$x_{i,t+1} = (1-g_i)s_i x_{i,t} + \frac{g_i \lambda_i x_{i,t}}{1+\sum_j a_{ij} g_j x_{j,t}} := x_{i,t} F_i(x)$$

For illustrative purposes, we focus on the model parametrized to the ambient rain scenario for a subset of species: *Acmispon wrangelianus*, *Hordeum murinum*, and *Plantago erecta* (parameters in Appendix A). First, we create the Community Disassembly Graph for the community. To do this, we find all coexistence states analytically (see Appendix B). Each species by itself persists at a globally stable equilibrium. Only one pair of species (*A. wrangelianus* and *H. murinum*) can coexist and when they do, they coexist at a globally-attracting state (Appendix B). Finally, we use the invasion graph approach to prove all three species can coexist in the sense of permanence (Hofbauer and Schreiber, 2022).

Next, we evaluate each species' IGR at each coexistence state. Since each coexistence state corresponds to a globally-stable equilibrium $x^* = (x_1^*, x_2^*, x_3^*)$, we can solve for the IGR analytically at the equilibrium. The IGR of species i at this equilibrium equals

$$\ln F_i(x^*) = \ln\left((1-g_i)s_i + \frac{g_i \lambda_i}{1+\sum_j a_{ij} g_j x_j^*}\right)$$

Using these IGRs, we identify all $-i$ communities and compute the Community Disassembly Graph (Figure 1A).

This Community Disassembly Graph identifies two secondary extinction events: the secondary extinction of *A. wrangelianus* following the loss of *H. murinum* and the secondary extinction of *P. erecta* following the loss of *A. wrangelianus* (Figure 1A). For illustrative purposes, we will focus on understanding why *P. erecta* goes extinct following the extinction of *A. wrangelianus*. To determine the cause of the secondary extinction event, we examine (1) what factors prevent *P. erecta* from establishing when only *H. murinum* is present and (2) what factors allow *P. erecta* to invade when *A. wrangelianus* is present in the community with *H. murinum*. Specifically, the factors of interest are competition against *P. erecta*, indirect impacts of competition between *A. wrangelianus* and *H. murinum* on *P. erecta* , and interactive effects between these direct and indirect effects.

P. erecta has a negative IGR at the *H. murinum* community (i.e., the -*A. wrangelianus*

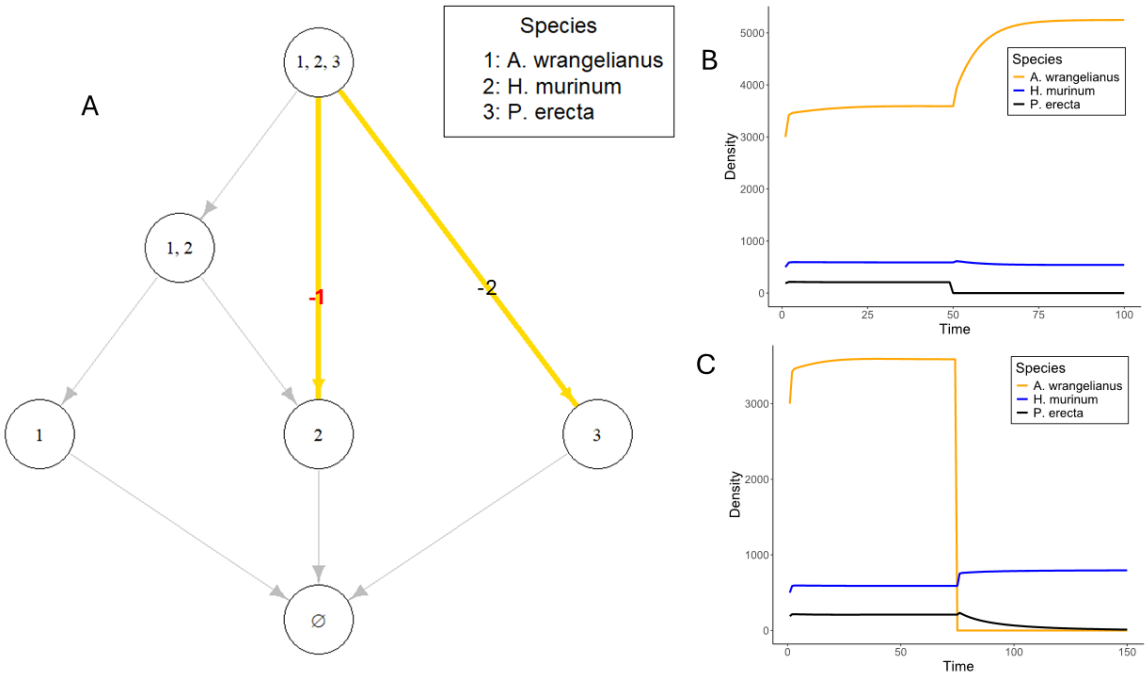

Figure 1: (A) Community Disassembly Graph of the annual plant community. Vertices depict coexisting subcommunities. Directed edges represent transitions from one community to another due to extinction of the labeled species. Extinctions resulting in no secondary extinctions are denoted by grey directed edges with no edge label while those containing secondary extinctions are in yellow with a corresponding edge label. The secondary extinction of interest is denoted by a red edge label. (B) Simulation of community dynamics following extinction of *P. erecta* at time step 50. Note that there are no secondary extinction events, matching the -*P. erecta* predicted in the Community Disassembly Graph. (C) Simulation of community dynamics following extinction of *A. wrangelianus* at time step 75. *P. erecta* decays towards extinction following the extinction of *A. wrangelianus*, confirming the secondary extinction predicted on the Community Disassembly Graph.

community), as it undergoes a secondary extinction following removal of *A. wrangelianus*. Our decomposition of this IGR (Figure 2) shows, as expected, the direct impact of competition from *H. murinum* on *P. erecta* is why this IGR is negative.

To understand why *P. erecta* can invade with *H. murinum* only in the presence of *A. wrangelianus*, we decompose its IGR at the *A. wrangelianus*–*H. murinum* community i.e. the $-$ *P. erecata* community. Individually, the direct impacts of competition from *H. murinum* and *A. wrangelianus* have large negative impacts on the IGR of *P. erecta* (second and third peach bars from the top in Figure 2). These negative impacts, however, are substantially reduced by the non-additive effects of competition on *P. erecta* and the indirect effects of these resident species competing. Importantly, this relatively small increase of direct competition is overcompensated by competition between *A. wrangelanius* and *H. murinum* having a positive effect on *P. erecta*

(positive peach bars). The competition between *P. erecta*'s two competitors and subadditivity of competition against *P. erecta* ultimately drives the IGR to be positive, allowing for successful invasion and, in this case, coexistence.

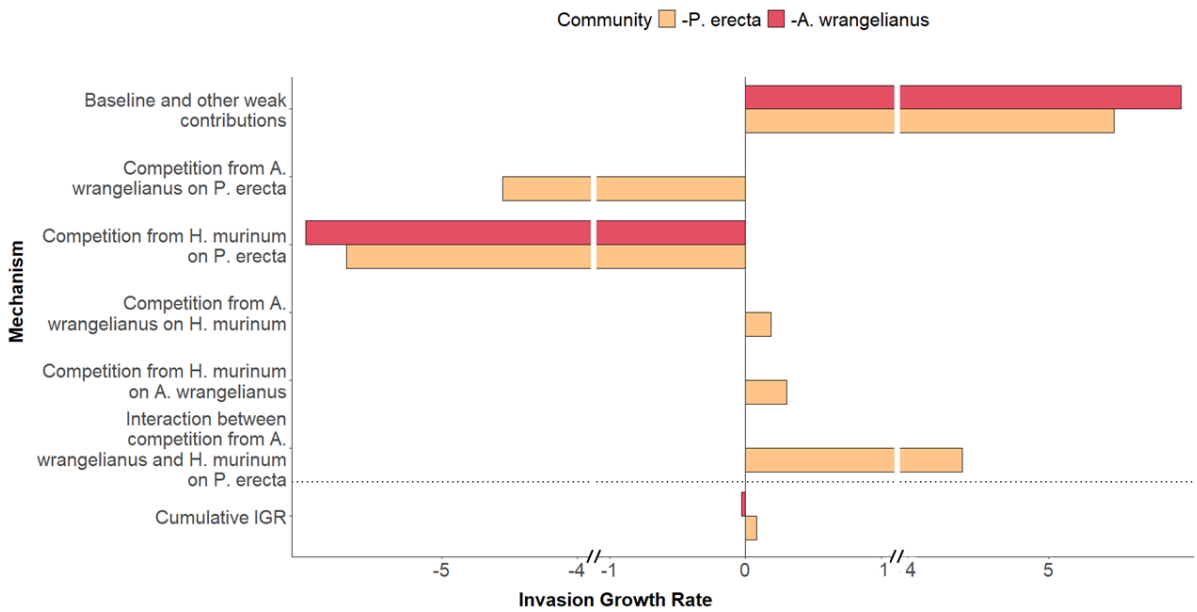

Figure 2: Decomposition of *P. erecta*'s IGR at the $-$*P. erecta* and $-$*A. wrangelianus* communities. The sum of all bars of a respective color above the dotted line will add to the value of the bar below the dotted line of the respective color. Mechanisms whose value is less than 0.01 were lumped into the baseline bar. Mechanisms not present in the $-i$ community have no contribution to the IGR and thus have no bar represented.

This analysis identifies the cause of *P. erecta*'s secondary extinction. In the community with *H. murinum* and *A. wrangelianus*, competition between *H. murinum* and *A. wrangelianus* suppresses their competitive dominance over *P. erecta*, permitting *P. erecta* to coexist within the full community. Consequently, the extinction of *A. wrangelianus* removes this competitive suppression of *H. murinum*, allowing *H. murinum* to competitively exclude *P. erecta*.

3.2 Facilitation

Facilitation can buffer species' densities against negative interactions such as predation (Glynn, 1976; Stachowicz and Hay, 1999) and competition (Pennings and Callaway, 1996; Stachowicz, 2001). However, reliance on facilitative or mutualist interactions for persistence can increase vulnerability to secondary extinctions (Aslan et al., 2013; Vanbergen et al., 2017).

For instance, Geijzendorffer et al. (2011) empirically parametrized a series of Lotka-Volterra models to a grassland system exhibiting both competitive and facilitative interactions. In these models, each species i has an intrinsic rate of growth, r_i, and a per-capita impact a_{ji} on species j. If a_{ji} is negative, species i has a competitive effect on species j while if positive, species i facilitates species j. The model is

$$\frac{dx_i}{dt} = x_i \left(r_i + \sum_j a_{ij} x_j \right) := x_i f_i(x)$$

For simplicity, we focus on the parameterization for spring in Appendix C and consider a subset of species: *Agrostis stolonifera*, *Lolium perenne*, *Phleum pratense*, *Trifolium pratense*, and *Trifolium repens*.

Using the invasion graph method (Hofbauer and Schreiber, 2022), we identify all coexistence states of the model. All of these coexistence states are not only local attractors, but global attractors i.e. permanent communities. Next, we evaluate the IGR of each species at each coexistence state. Due to the time averaging property of Lotka-Volterra models (Hofbauer and Sigmund, 1998), we can analytically solve for each IGR by evaluating at the respective equilibrium $x^* = (x_1^*, \ldots, x_5^*)$ i.e.,

$$f_i(x^*) = r_i + \sum_j a_{ij} x_j^*$$

Using this information, we computed the Community Disassembly graph (Figure 3A). This analysis reveals that all five species coexist and the existence of eight possible secondary extinctions events. Half of the secondary extinction events occur following the extinction of *T. repens* which causes the secondary extinction of *T. pratense*. This suggests that *T. repens* plays a crucial role in allowing *T. pratense* to coexist with other species in multiple contexts.

To understand these secondary extinctions, we focus on the secondary extinction of *T. pratense* when *T. repens* is removed from the entire community. To understand why this secondary extinction event occurs, we must address two key questions: (1) what factors prevent *T. pratense* from successfully invading the community with *A. stolonifera*, *L. perenne*, and *P. pratense* (i.e., in the -*T. repens* community), and (2) what factors allow *T. pratense* to success-

fully invade the community with these species if *T. repens* is present (i.e., in the -*T. pratense* community)? Specifically, we quantify the contributions of species interactions on the IGR of *T. pratense* relative to its impact on *T. pratense*'s competitors. We can group species interactions of interest into four categories: the direct effects of competition and facilitation on *T. pratense* and the indirect effects of competition and facilitation on competitors of *T. pratense*.

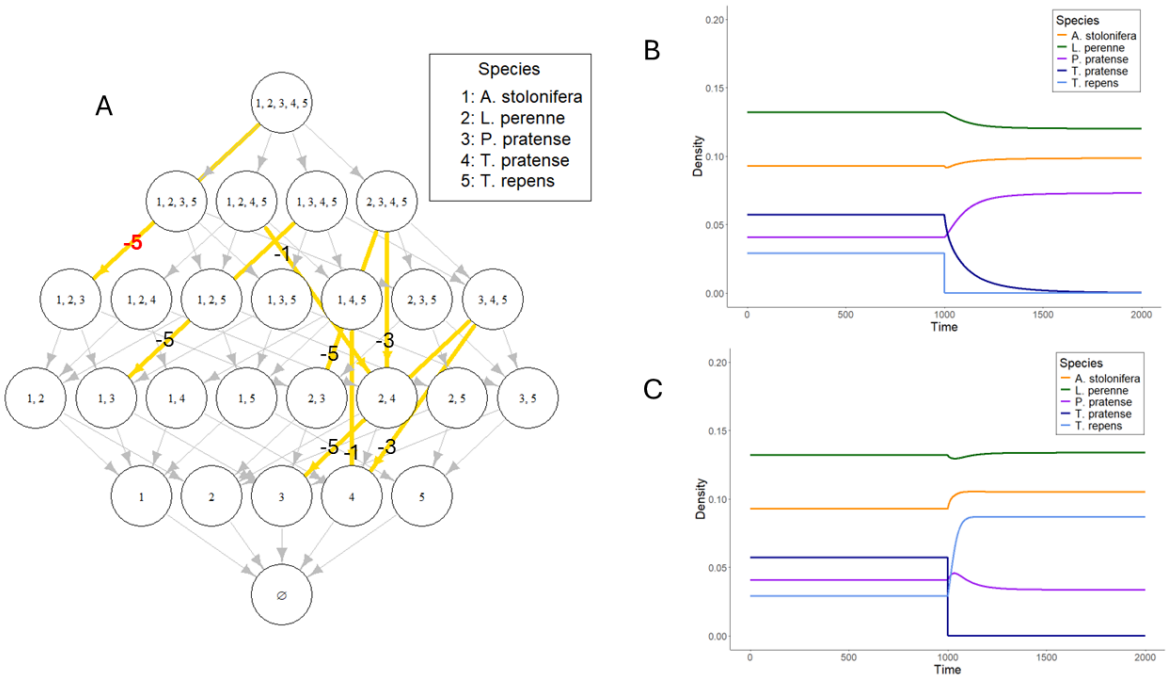

Figure 3: (A) Community Disassembly Graph of the grassland community. Vertices depict coexisting subcommunities. Directed edges represent transitions from one community to another due to extinction of the labeled species. Extinctions resulting in no secondary extinctions are denoted by grey directed edges with no edge label while those containing secondary extinctions are in yellow with a corresponding edge label. The secondary extinction of interest is denoted by a red edge label. (B) Simulation of community dynamics following extinction of *T. repens* at time step 1000. *T. pratense* decays towards extinction following the extinction of *T. repens*, confirming the secondary extinction predicted on the Community Disassembly Graph. (C) Simulation of community dynamics following extinction of *T. pratense* at time step 1000. Note that there are no secondary extinction events, matching the -*T. pratense* predicted in the Community Disassembly Graph.

To understand why *T. pratense* can not establish in the $-$*T. pratense* community, we decompose its negative IGR when the other species are equilibrium. We find that direct effects of competition and the indirect effects of facilitation among the competitors outweigh the indirect effects of competition among competitors. This results in a negative IGR for *T. pratense*. However, without the indirect effect of facilitation amongv competitors, the IGR would be positive. Hence, facilitation among the competitors plays a crucial role on the competitive exclusion of

T. pratense.

Next we examine how the presence of *T. repens* permits the establishment of *T. pratense*. Unlike in the $-$*T. repens* community, direct facilitation on *T. pratense* confers a significant, positive contribution to its IGR. Additionally, competition against *T. pratense* is less harsh in the $-$*T. pratense* community than in the $-$*T. repens* community. In the $-$ *T. pratense* community, indirect effects due to competition and facilitation are stronger. However, as they have opposing effects on the IGRs of the same magnitude, the net impact of these indirect effects are negligible on *T. pratense*'s IGR. These mechanisms allow for *T. pratense* to have a positive IGR in the $-$*T. pratense* community unlike in the $-$*T. repens* community.

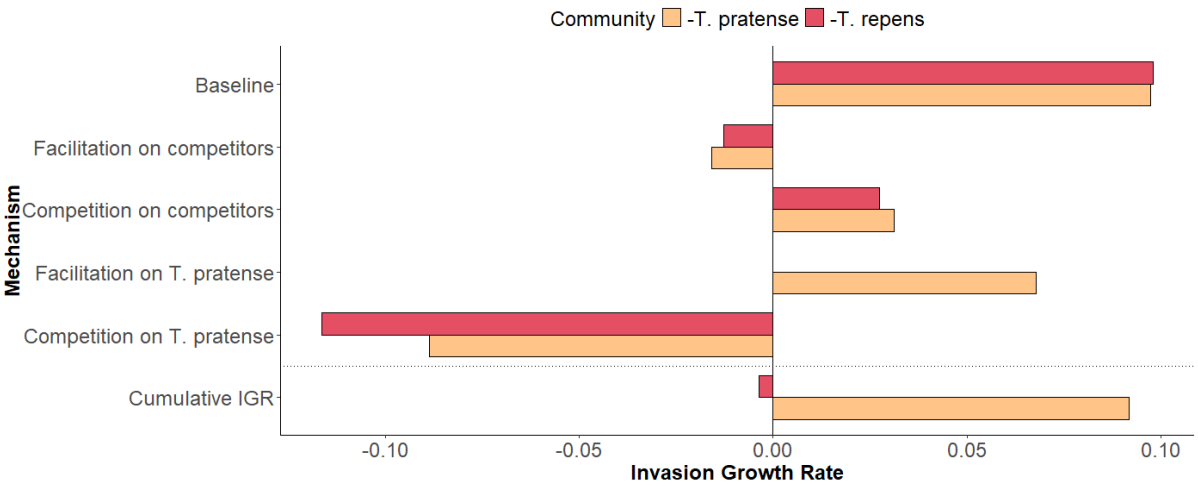

Figure 4: Decomposition of *T. pratense*'s IGR at the $-$*T. pratense* and $-$*T. repens* communities. The sum of all bars of a respective color above the dotted line will add to the value of the bar below the dotted line of the respective color. Mechanisms not present in the $-i$ community have no contribution to the IGR and thus have no bar represented.

These decompositions imply that the secondary extinction of *T. pratense* following loss of *T. repens* was primarily driven by the loss of facilitation and weakened competition against competitors of *T. pratense*. In the full community, *T. repens*'s facilitation permits *T. pratense* to persist despite competitive pressures. However, following the extinction of *T. repens*, *T. pratense* becomes unable to withstand the competition from the remaining species in the disassembled community due to the indirect effect of facilitation amongst its competitors.

3.3 Predation

Predation can maintain coexistence by regulating competitively dominant prey species– an effect known as keystone predation (Paine, 1966; Letnic et al., 2009; Wallach et al., 2015). A well-studied model of keystone predation is the diamond model with a basal resource (R), two competitors (C_1 and C_2) competing for the basal resource, and a top predator (P) that preys upon both competitors (McCann et al., 1998; Schreiber and Rittenhouse, 2004; Vasseur and Fox, 2007; Shoemaker et al., 2020). Following Vasseur and Fox (2007)'s model formulation and parameterization in Appendix D, the dynamics are

$$
\begin{aligned}
\frac{dP}{dt} &= -M_P P + J_P P \frac{\Omega_{PC_1} C_1 + (1-\Omega_{PC_1}) C_2}{\Omega_{PC_1} C_1 + (1-\Omega_{PC_1}) C_2 + C_0} \\
&:= P \cdot f_P(R, C_1, C_2, P) \\
\frac{dC_1}{dt} &= -M_{C_1} C_1 + \Omega_{C_1 R} J_{C_1} C_1 \frac{R}{R + R_{0_1}} - J_P P \frac{\Omega_{PC_1} C_1}{\Omega_{PC_1} C_1 + (1-\Omega_{PC_1}) C_2 + C_0} \\
&:= C_1 \cdot f_{C_1}(R, C_1, C_2, P) \\
\frac{dC_2}{dt} &= -M_{C_2} C_2 + \Omega_{C_2 R} J_{C_2} C_2 \frac{R}{R + R_{0_2}} - J_P P \frac{(1-\Omega_{PC_1}) C_2}{\Omega_{PC_1} C_1 + (1-\Omega_{PC_1}) C_2 + C_0} \\
&:= C_2 \cdot f_{C_2}(R, C_1, C_2, P) \\
\frac{dR}{dt} &= rR\left(1 - \frac{R}{K}\right) - \Omega_{C_1 R} J_{C_1} C_1 \frac{R}{R + R_{0_1}} - \Omega_{C_2 R} J_{C_2} C_2 \frac{R}{R + R_{0_2}} \\
&:= R \cdot f_R(R, C_1, C_2, P)
\end{aligned}
$$

Due to the complexity of the model, we use numerical simulations to identify all coexistence states. For each subset of species, we run a set of simulations with each of those species at initially positive densities. We run the dynamics until they reach stationarity and identify which species successfully coexist. We define coexistence as all species at initially positive density having an average density greater than 10^{-9} after the burn-in period at $t = 1{,}000$ to the end of the time series. For each set of species, we test multiple sets of initial conditions to identify other attractors if they exist. For this parameterization, we only identified at most one attractor for each coexisting subsystem.

To calculate the IGR for a given coexistence state, we numerically integrated the model using the deSolve package in the programming language R (Soetaert et al., 2010) evaluated at time intervals of $\Delta t = 0.1$ with a burn-in time of $1,000$ and a total run time of $10,000$. We approximate the IGR for species i

$$\lim_{T\to\infty} \frac{1}{T} \int_{t=0}^{T} f_i(R(t), C_1(t), C_2(t), P(t))dt$$

by the Riemann sum

$$\sum_{k=10,000}^{100,000} f_i(R(k\Delta t), C_1(k\Delta t), C_2(k\Delta t), P(k\Delta t))\Delta t$$

for $i \in \{R, C_1, C_2, P\}$.

Using the numerically identified coexistence states and the associated IGRs, we calculate the model's Community Disassembly Graph. Under the parametrization studied in Vasseur and Fox (2007) and Shoemaker et al. (2020), we find several secondary extinctions (Figure 5A). Most of the secondary extinctions are intuitive (loss of resource leads to loss of species directly dependent on the resource). However, two are more interesting: extinction of the predator P induces secondary extinction of the second consumer C_2 and the extinction of the first consumer C_1 induces the secondary extinction of the predator P. Here, we study how the extinction of P induces the secondary extinction of C_2. We choose to investigate three ecological factors: relative nonlinearity in response to resource fluctuations, predator preference (Ω_{PC_1}), and the resident consumer's utilization of the shared resource (J_{C_1}).

First, we assess why consumer 2 C_2 has a negative IGR in the community with only the resource R and the other consumer C_1. As expected, the utilization of the resource by C_1 is the primary factor that makes C_2's IGR negative (fourth red bar in Figure 6). We find that fluctuations in R have a negative impact on the IGR of C_2, but that the interaction between fluctuations in R and C_1's intake of R has a positive impact on C_2's IGR due to its negative impact on C_1. This positive contribution, however, does not offset the negative contributions of each factor independently, resulting in a negative IGR of C_2.

Next, we examine why C_2 can establish in the presence of the predator P. To do this, we

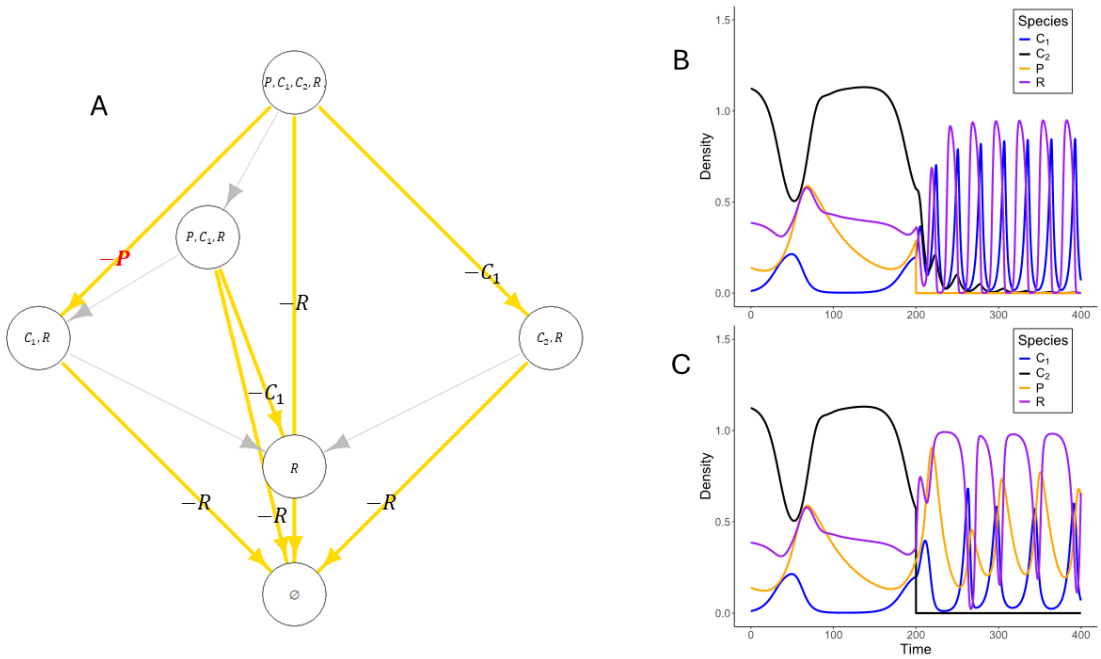

Figure 5: (A) Community Disassembly Graph of the diamond model. Vertices depict coexisting subcommunities. Directed edges represent transitions from one community to another due to extinction of the labeled species. Extinctions resulting in no secondary extinctions are denoted by grey directed edges with no edge label while those containing secondary extinctions are in yellow with a corresponding edge label. The secondary extinction of interest is denoted by a red edge label. (B) Simulation of community dynamics following extinction of P at time step 200. C_2 decays towards extinction following the extinction of P, confirming the secondary extinction predicted on the Community Disassembly Graph. (C) Simulation of community dynamics following extinction of C_2 at time step 200. Note that there are no secondary extinction events, matching the -C_2 predicted in the Community Disassembly Graph.

decompose the IGR of C_2 at the $-C_2$ community. Decomposing the IGR of C_2, we find that, yet again, fluctuations in R and C_1's use of R have negative contributions to the IGR while their interaction has a weak, positive contribution (peach bars in 6). The effect of predator preference is sufficiently positive to counteract the negative contributions of fluctuations in R and C_1's utilization of R. This confirms our hypothesis that successful invasion of C_2 is dependent on P's presence and, crucially, its preference for consuming C_1.

Comparing the two IGR decompositions, we find that the predator's presence made baseline conditions and resource fluctuations more beneficial for C_2 while making the impact of C_1's resource utilization and the interaction between these factors more detrimental for C_2. In addition to changing these pre-existing factors, the predator's preference serves as a novel, positive factor resulting in a positive IGR.

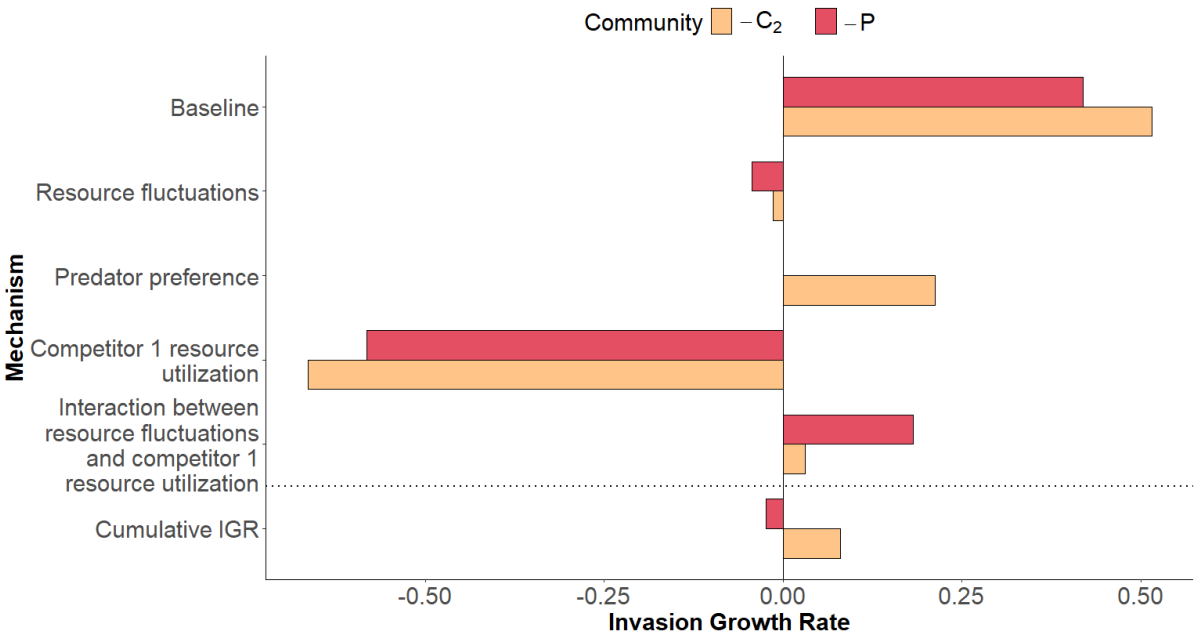

Figure 6: Decomposition of C_2's IGR at the $-C_2$ and $-P$ communities. The sum of all bars of a respective color above the dotted line will add to the value of the bar below the dotted line of the respective color. Mechanisms not present in the $-i$ community have no contribution to the IGR and thus have no bar represented.

Synthesizing this information, when P is present, its preferential consumption of C_1 sufficiently suppresses C_1's competitive dominance over C_2, enabling coexistence of all species. However, the extinction of P eliminates the top down control on C_2. Without this top-down control, C_1's utilization of R made it a superior competitor, leading to competitive exclusion of C_2. Thus, C_2's coexistence in the full community is dependent upon P's presence, implying that extinction of P would drive a subsequent loss of C_2.

4 Discussion

While IGRs have traditionally been used to identify mechanisms of species coexistence, they are increasingly applied to a broader range of ecological phenomena, including priority effects (Ke and Letten, 2018; Grainger et al., 2019a), competitive exclusion (Germain et al., 2018; Shoemaker et al., 2020), and community assembly (Spaak and Schreiber, 2023; Song and Spaak, 2024). We contribute to this expanding body of work by extending key concepts from Modern Coexistence Theory such as IGRs and $-i$ communities to the study of community disassembly. In doing so, we use IGRs to identify secondary extinctions, further demonstrating

their utility beyond coexistence analysis (Grainger et al., 2019b).

Our approach to community disassembly relies on an underappreciated cornerstone of Modern Coexistence Theory: $-i$ communities. These communities, introduced by Chesson (1994), correspond to the ecological dynamics that emerge when species i is absent (or very rare). The community disassembly graph introduced here simply uses this concept recursively, thus describing the cascading effects of a sequence of species losses. Because community disassembly graphs are characterized by invasion growth rates, they are the natural counterpart of invasion graphs that describe the possible consequences of invasions by one or multiple species on community structure (Hofbauer and Schreiber, 2022; Spaak and Schreiber, 2023; Godoy et al., 2024; Schreiber, 2025). Moreover, invasion graphs confirm, in a mathematically rigorous manner, an intuitive assumption underlying Modern Coexistence Theory: coexistence (in the sense of permanence) requires that each species has a positive invasion growth rate (IGR) in its $-i$ communities (Grainger et al., 2019a). As illustrated in our applications, secondary extinctions lead to $-i$ communities where multiple species, not only species i, are missing. However, almost all theoretical developments and applications of MCT focus on species whose loss does not lead to secondary extinctions (MacArthur and Levins, 1967; Chesson, 1994; Ellner et al., 2019; Shoemaker et al., 2020).This limitation suggests that MCT frameworks must be expanded to account for systems where species losses trigger cascading extinctions.

Most studies of community disassembly focus on the overall robustness of ecological communities to extinction events (Dunne et al., 2002a; Keyes et al., 2024), adopting a broad-scale perspective on the drivers of disassembly. In contrast, we take a fine-scale approach by examining individual cases of secondary extinction, allowing for identification of specific underlying mechanisms. By leveraging decomposition techniques from Modern Coexistence Theory at $-i$ communities with secondary extinctions, we identify the ecological drivers of these events and extend the utility existing coexistence techniques (Chesson, 1994; Ellner et al., 2019).

The applications presented demonstrate that secondary extinctions can arise from multiple mechanisms. In the annual plant model (Figure 2), the persistence of *P. erecta* in the presence of *A. wrangelianus* and *H. murinum* depends on both direct competition between the two species and the saturating competitive effects of *H. murinum* and *A. wrangelianus* against *P. erecta*.

Without either factor, *P. erecta* would be unable to coexist with *A. wrangelianus* and *H. murinum*. Similarly, in the grassland system (Figure 4), the secondary extinction of *T. pratense* was driven by both increased direct competition and the loss of direct facilitation in the disassembled community. These findings support prior studies suggesting that ecological mechanisms and stressors can interact in both additive and synergistic ways to influence the likelihood of secondary extinctions (Graham et al., 2011; Colwell et al., 2012; Brodie et al., 2014).

A possible secondary extinction scenario not considered here is that the $-i$ community of the secondarily extinct species might not contain all species in the full community except species i; though, the disassembled community might still be able to access the full community through single-species invasions. If one is interested in how the full community reassembles back to the pre-extinction state, one can decompose the IGR of the secondarily extinct species at the disassembled community and then decompose the IGRs of invading species moving along an assembly path from the disassembled community to the full community. We present an analysis of this in the annual plant model from Van Dyke et al. (2022) in Appendix E.

5 Challenges and future directions

Our study uses IGRs at multiple communities to understand mechanisms driving secondary extinctions. This approach allows us to understand both how the secondarily extinct species coexists in the full community and why it is excluded in the disassembled community. However, the utility of this procedure extends beyond processes of disassembly. For example, in community assembly, the successful invasion of a species from the regional pool might displace resident species (Horn, 1974; Wainright et al., 2021; Zhou et al., 2023). Since the invading species could invade when rare, we know it must have a positive IGR at the pre-invasion community. Furthermore, since the resident species was displaced following introduction of the invading species, we know it must have a negative IGR at the post-invasion community (Schreiber, 2025). Thus, a similar procedure can be followed: decompose the species' IGR in its own $-i$ community to understand how it can invade it to reach the pre-invasion community and decompose its growth rate in the post-invasion community to determine what new attributes

of the system drive exclusion following introduction of the new species.

One limitation of this study is its focus on secondary extinctions in communities that are accessible through single-species invasion events. A classic example of a coexisting community that cannot be assembled through single-species invasions are rock-paper-scissors communities (May and Leonard, 1975). In this model, no two species can coexist since one always outcompetes the other; however, all three species can coexist together. If an extinction event occurs in the full community, there will be a secondary extinction event since no pair of species can coexist. Consequently, there is no way to go from the disassembled community back to the full community through single-species invasions. Similar dynamics can manifest in higher-dimensional communities (Hofbauer, 1994; Schreiber, 1998; Schreiber and Rittenhouse, 2004; Allesina and Levine, 2011), leaving species susceptible to secondary extinction (Schreiber, 1998; Vandermeer, 2024). Mathematical methods for handling many of these intransitivities have existed for decades (Hofbauer, 1981; Schreiber, 2000). Although rooted in invasion growth rates, these methods have only recently been incorporated into an MCT partitioning framework for the classical three-species models (Ranjan et al., 2024). These advances hint at the possibility of modifying our framework to account for secondary extinctions in intransitive systems.

Another limitation is that MCT techniques are often uninformative when species exhibit Allee effects, where growth is negative at low densities (Barabás et al., 2018). In our case, while the identification of secondary extinctions is not affected by Allee effects, explaining why a species with an Allee effect goes secondarily extinct requires different methods. This is because such species have negative IGRs in their $-i$ community and consequently cannot return to the pre-extinction community through low-density introductions (Spaak and Schreiber, 2023), rendering the decomposition of low-density growth rates uninformative for assessing full coexistence of the system. However, in some cases, alternatives to IGRs exist for identifying when and why coexistence occurs (Schreiber et al., 2019; Ellner et al., 2022), which raises the possibility that they could be adapted to understand the causes of secondary extinctions.

By applying MCT to community disassembly, we introduce a novel framework to identify secondary extinctions and quantify the underlying driving ecological factors. Moreover, we demonstrate that decomposing IGRs at multiple communities can is necessary to understand

the directionality and relative importance of the underlying ecological factors. Given the utility of these approaches, we believe similar approaches are promising for future studies of not only community disassembly but also coexistence and community assembly.

6 Author Contributions

J. Brennan and S.J Schreiber conceived the idea. JB performed the computational analyses, created the figures, and drafted the manuscript with feedback from SJS. SJS performed the mathematical analyses with feedback from JB. JB and SJS reviewed and edited manuscript drafts.

7 Acknowledgments

We would like to thank Marissa Baskett and and John Stachowicz for comments on an early draft. We would also like to thank Raissa D'Souza, Alan Hastings, and Marcel Holyoak for feedback throughout the development of this project. JB was supported by the National Science Foundation Graduate Research Fellowship program under Grant No. DGE-2439024.

A Parameters for competition in annual plant community

The annual plant model is given by

$$x_{i,t+1} = (1 - g_i)s_i x_{i,t} + \frac{g_i \lambda_i x_{i,t}}{1 + \sum_j a_{ij} g_j x_{j,t}} \tag{1}$$

Here, we represent competition coefficent a_{ij} as the i-th row and j-th column in the matrix A and g_i, λ_i, and s_i as the i-th element in the vectors $\vec{g}$, $\vec{\lambda}$, and $\vec{s}$, respectively. Under this notation, the parameters are given by

$$A = \begin{bmatrix} 0.27290462 & 0.9415389 & 0.5590646 \\ 0.13755487 & 0.9483990 & 0.1599514 \\ 0.08483079 & 1.0221670 & 0.4161495 \end{bmatrix}$$
$$\vec{g} = \begin{bmatrix} 0.2240310 & 0.6666667 & 0.6029647 \end{bmatrix}$$
$$\vec{\lambda} = \begin{bmatrix} 2351.5366 & 745.9973 & 654.6758 \end{bmatrix}$$
$$\vec{s} = \begin{bmatrix} 0.2625463 & 0.0450000 & 0.6215016 \end{bmatrix}$$

where species $1, 2,$ and 3 are *A. wrangelianus*, *H. murinum*, and *P. erecta*, respectively.

B Global dynamics of the annual plant model

To identify all the community attractors of the annual plant model (1) with three species, we analyze the two subsystems of species using the theory of monotone dynamical systems (Smith, 1995), specifically results for competitive planar maps (Smith, 1998). Then we use invasion graphs (Hofbauer and Schreiber, 2022; Schreiber, 2025) to verify the existence of an attractor that supports all three species.

B.1 Global dynamics of species pairs

We begin by characterizing the dynamics of any pair of species. Without loss of generality, say $i = 1, 2$. Define the update mapping $P(x) = (P_1(x), P_2(x))$ by

$$P_1(x) = x_1 \left(\frac{\lambda_1}{1 + \alpha_{11}x_1 + \alpha_{12}x_2} + s_1 \right) \text{ and } P_2(x) = x_2 \left(\frac{\lambda_2}{1 + \alpha_{21}x_1 + \alpha_{22}x_2} + s_2 \right).$$

We use results from (Smith, 1998) to characterize the global dynamics. This requires using the theory of monotone maps. The relevant terminology is described in Smith (1995, 1998). First, we verify that (1) with two species ($i = 1, 2$) is strictly competitive in the positive quadrant $(0, \infty)^2$. By Proposition 2.1 in (Smith, 1998) it is sufficient to show that P_1 (respectively, P_2) is a strictly increasing function of x_1 and a strictly decreasing function of x_2 (respectively, strictly increasing in x_2 and strictly decreasing in x_1. To this end, we compute the partial derivatives of F_1 and F_2 with respect to x_1 and x_2:

$$\begin{aligned}
\frac{\partial P_1}{\partial x_1} &= \frac{\lambda_1(1 + \alpha_{12}x_2)}{\Delta_1^2} + s_1 \quad \frac{\partial P_1}{\partial x_2} = -\frac{\alpha_{12}\lambda_1 x_1}{\Delta_1^2} \\
\frac{\partial P_2}{\partial x_1} &= -\frac{\alpha_{21}\lambda_2 x_2}{\Delta_2^2} \quad \frac{\partial P_2}{\partial x_2} = \frac{\lambda_2(1 + \alpha_{21}x_1)}{\Delta_2^2} + s_2 \\
\text{where } \Delta_1 &= 1 + \alpha_{11}x_1 + \alpha_{12}x_2 \text{ and } \Delta_2 = 1 + \alpha_{21}x_1 + \alpha_{22}x_2.
\end{aligned}$$

As the partial derivatives $\frac{\partial P_i}{\partial x_i}$ are strictly positive in $[0, \infty)^2$ for $i = 1, 2$, the functions F_i increase strictly in x_1 in $[0, \infty)^\infty$. As the partial derivatives $\frac{\partial P_i}{\partial x_j}$ for $i \neq j$ are negative in $(0, \infty)^2$, the functions F_i strictly decrease in x_j ($j \neq i$) in the positive quadrant $(0, \infty)^2$. Hence, by Proposition 2.3 in (Smith, 1998) , (1) is strictly competitive in the positive quadrant.

Next, we verify hypothesis (H+) in (Smith, 1998) for P on $A = (0, \infty)^2$. This hypothesis consists of four conditions (a)–(d). Condition (a) holds immediately for the competitive ordering $<_K$ on A. Condition (b) requires that the determinant of the Jacobian matrix

$$DP(x) = \begin{pmatrix} \frac{\partial P_1}{\partial x_1} & \frac{\partial P_1}{\partial x_2} \\ \frac{\partial P_2}{\partial x_1} & \frac{\partial P_2}{\partial x_2} \end{pmatrix}$$

is positive in $(0,\infty)^2$. The following calculation ensures that this condition is satisfied:

$$\begin{aligned}
\Delta_1^2\Delta_2^2\det(DP(x)) &= \lambda_1\lambda_2(1+\alpha_{12}x_2)(1+\alpha_{21}x_1)+s_1(1+\alpha_{21}x_1)\Delta_2+s_2(1+\alpha_{12}x_2)\Delta_1+s_1s_2\Delta_1\Delta_2 \\
&\quad -\lambda_1\lambda_2\alpha_{12}\alpha_{21}x_1x_2 \\
&= \lambda_1\lambda_2(1+\alpha_{12}x_2+\alpha_{21}x_1)+s_1(1+\alpha_{21}x_1)\Delta_2+s_2(1+\alpha_{12}x_2)\Delta_1+s_1s_2\Delta_1\Delta_2
\end{aligned}$$

The third condition (c) requires that the diagonal entries of $DP(x)$ be strictly positive and the off-diagonal elements be strictly negative on $(0,\infty)^2$. This follows immediately from our partial derivative calculations. The final condition (d) requires that P is injective in $(0,\infty)^2$. As $\det(DP(x)) > 0$ on $[0,\infty)^2$ and $[0,\infty)^2$ is connected, all points in $(0,\infty)^2$ have the same number of preimages. As the only preimage of $(0,0)$ is $(0,0)$, it follows that P is injective.

Having verified these conditions, Corollary 4.4 in (Smith, 1998) implies that all trajectories of (B) for $i = 1,2$ converge to an equilibrium. To understand which initial conditions converge to which equilibria, we need to solve the equilibria and check the invasion criteria at these equilibria. As we describe below, there is generically (in particular, for our parameters) at most one equilibrium for any subset of species. Moreover, for any pair of species in the parameterized model, only one of two mutual invasibility conditions hold. Either both species have a positive invasion growth rate at the other species equilibrium or the invasion growth rates are of oppositie sign. When the former occurs, the single species equilibria are unstable (saddles), and there is a unique equilibrium, call it x^*, supporting the other two species, i.e. $x_1^* > 0$ and $x_2^* > 0$. Therefore, any trajectory where initially both species have positive densities converges to x^* i.e. x^* is globally stable. Alternatively, suppose that the invasion growth rates have opposite signs. Without loss of generality, say the invasion growth rate of species 2 is negative at the equilibrium $(x_1^*, 0)$ of species 1. Then there is no equilibrium supporting both species and the extinction equilibrium $(0,0)$ and species 2 equilibrium $(0, x_2^*)$ are unstable, while the species 1 equilibrium is stable. Therefore, Corollary 4.4 implies that all trajectories at which species 1 is initial present converge to $(x_1^*, 0)$. These results fully characterize the dynamics of all the two species pairs in the three species parameterized model.

B.2 Three species coexistence

To verify coexistence of the three species, we use the invasion graph approach to verify coexistence in the sense of permanence. This approach was introduced for differential equations in (Hofbauer and Schreiber, 2022) and extended to flow-kick models that include difference equations in (Schreiber, 2025). Calculating the equilibria as detailed below for all single and two species subsystems, as described below, and using the convergence results for the single and two species subsystems, one can verify that the invasion graph is acyclic and that the invasion growth rate of species i for $i = 1, 2, 3$ is positive at the $-i$ equilibria. Hence, Theorem 4.8 in (Schreiber, 2025) implies that all three species coexist in the sense of permanence. Numerical simulations suggest that permanence occurs via a global stable equilibrium.

B.3 Finding equilibria

To find the non-trivial equilibrium of the annual plant model with species $S = \{1, \ldots, n\}$, we require

$$1 = (1 - g_i)s_i + \frac{g_i \lambda_i}{1 + \sum_j a_{ij} g_j x_j^*}$$

for all species $i \in S$. Isolating the sum, we obtain

$$\frac{g_i \lambda_i}{1 - (1 - g_i)s_i} - 1 = \sum_j a_{ij} g_j x_j^*.$$

We define an $n \times n$ matrix M where $M_{ii} = g_i a_{ii}$ and $M_{ij} = a_{ij}$ for $i \neq j$. We also define a vector b where $b_i = \frac{g_i \lambda_i}{1-(1-g_i)s_i} - 1$. Then, the nontrivial equilibrium satisfies $x^* = M^{-1} b$.

C Parameters for facilitation in grassland community case study

The model for the grassland community is

$$\frac{dx_i}{dt} = x_i \left(r_i + \sum_j a_{ij} x_j \right) \tag{2}$$

If we represent the densities of each species as $\vec{x}$, we can represent the model as

$$\frac{d\vec{x}}{dt} = \vec{x} \odot (\vec{r} + A\vec{x}) \tag{3}$$

where $\odot$ is element-wise matrix multiplication. Under the parametrization from Geijzendorffer et al. (2011), the parameters for the model are

$$\vec{r} = \begin{bmatrix} 0.10077 & 0.04519 & 0.10343 & 0.11271 & 0.07652 \end{bmatrix}^T$$

$$A = \begin{bmatrix} -1.28 & 0.15 & 0.10 & -0.16 & 0.12 \\ 0.13 & -0.41 & -0.12 & 0.03 & 0 \\ -0.38 & -0.30 & -0.41 & -0.15 & -0.11 \\ -0.39 & -0.15 & -0.82 & -0.8 & 0.78 \\ -0.02 & -0.18 & -0.05 & -0.57 & -0.56 \end{bmatrix}$$

for *A. stolonifera*, *L. perenne*, *P. pratense*, *T. pratense*, and *T. repens*, respectively.

D Parameters for predation in diamond model

Here, we use the same parametrization as Vasseur and Fox (2007) and Shoemaker et al. (2020).

Parameter	Description	Value
r	Resource intrinsic rate of growth	1.0
K	Resource carrying capacity	1.0
J_{C_1}	Competitor 1's ingestion rate	0.8036
J_{C_2}	Competitor 2's ingestion rate	0.7
J_P	Predator ingestion rate	0.4
M_{C_1}	Competitor 1's intrinsic mortality rate	0.4
M_{C_2}	Competitor 2's intrinsic mortality rate	0.2
M_P	Predator's intrinsic mortality rate	0.08
R_{0_1}	Competitor 1's half saturation constant of the resource	0.16129
R_{0_2}	Competitor 2's half saturation constant of the resource	0.9
C_0	Predator's half saturation constant of the competitors	0.5
Ω_{PC_1}	Predator's prey preference for competitor 1	0.92
Ω_{C_1R}	Competitor 1's preference coefficient for the resource	1.0
Ω_{C_2R}	Competitor 2's preference coefficient for the resource	0.98

E Decomposition procedure at $-$secondarily extinct species community missing more species than the secondarily extinct species

Revisiting the annual plant model, there exists another secondary extinction event in the full community. As shown in Figure 1A, extinction of *H. murinum* leads to the secondary extinction of *A. wrangelianus*. As the procedure follows, we will (1) understand why *A. wrangelianus* is excluded by *P. erecta* and (2) why it can coexist with *P. erecta* if *H. murinum* is present.

Figure 1A shows that the -*A. wrangelianus* community has a secondary extinction event of *P. erecta*. Thus, introduction of *A. wrangelianus* alone cannot restore the pre-disassembled community. Thus, we identify a path from the -*A. wrangelianus community* back to the full community. For this empirical example, there exists only one path from -*A. wrangelianus* community to the full community: invasion of *A. wrangelianus* in -*A. wrangelianus* community

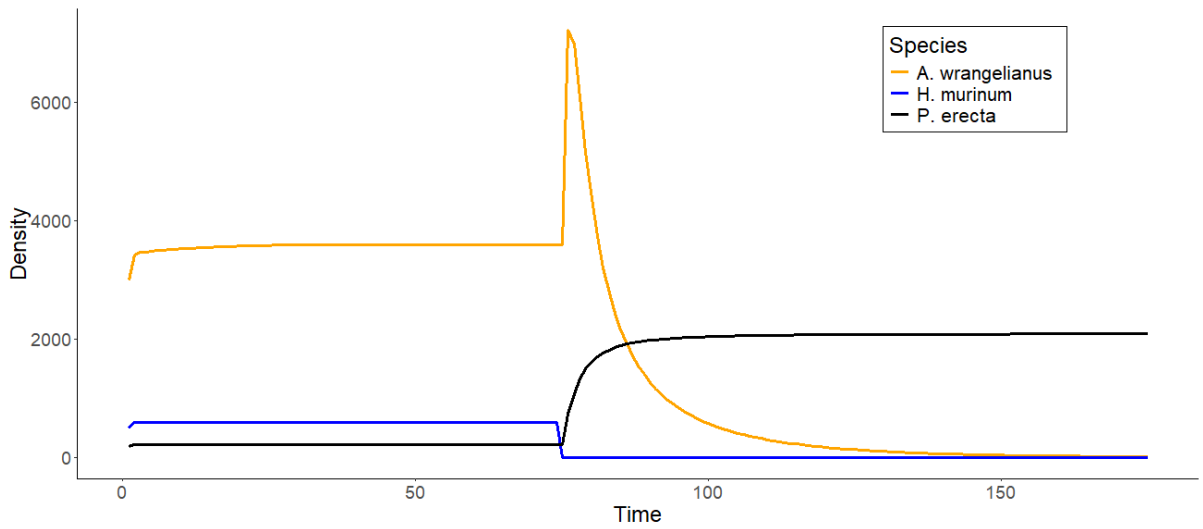

Figure 7: Simulation of community dynamics following extinction of *H. murinum* at time step 75. Note that this leads to a secondary extinction of *A. wrangelianus*, matching the -*H. murinum* predicted in the Community Disassembly Graph in Figure 1A.

that changes the composition to coexistence of *A. wrangelianus* and *H. murinum*, followed by invasion of *P. erecta* to reassemble the system back to the full community. Furthermore, the -*H. murinum* can access the -*A. wrangelianus* community through invasion of *H. murinum* displacing *P. erecta*, as we know from Figure 2A.

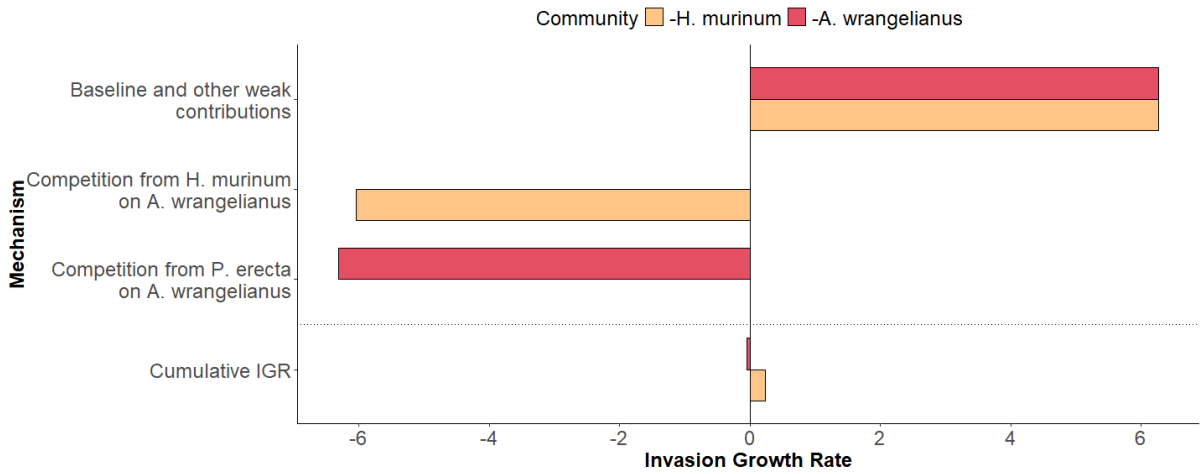

Figure 8: Invasion Growth

Along this assembly path, *A. wrangelianus* only needs to successfully invade once at the -*A. wrangelianus community* since it is not displaced by subsequent invasions on the assembly path. Thus, we simply decompose the invasion growth rate of *A. wrangelianus* at the -*A. wrangelianus* community to understand why it successfully invades in this community.

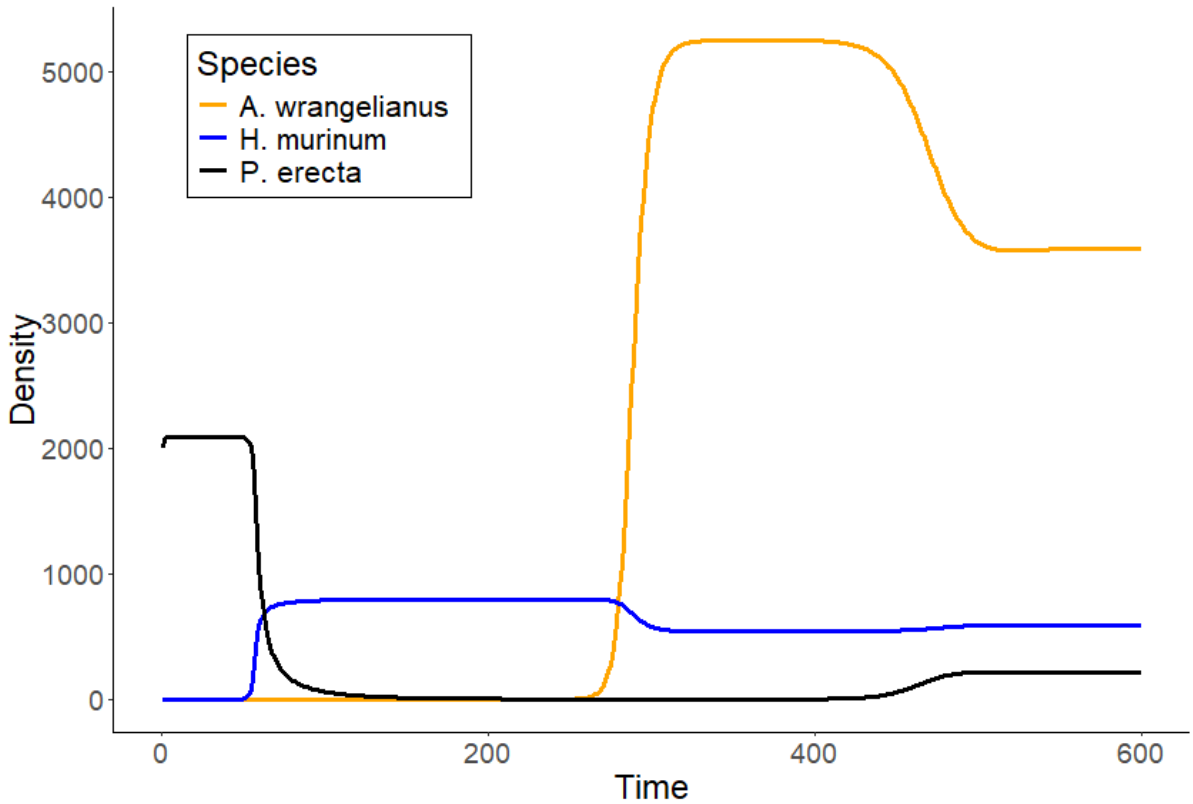

Figure 9: Simulation of dynamics associated with invasion. Invasion of *H. murinum* at time step 50; invasion of *A. wrangelianus* at time step 250; invasion of *P. erecta* at time step 400.

As shown in Figure 9, *A. wrangelianus* can invade the $-A.$ *wrangelianus* community, only containing *H. murinum*. Furthermore, since *H. murinum* has a positive invasion growth rate in the community only containing *A. wrangelianus*, we know they coexist through mutual invasibility.

To determine why *P. erecta* does not displace *A. wrangelianus* in the community with *H. murinum*, we can again decompose invasion growth rates. First, we identify all coexisting communities that are candidates for a post-invasion community following a displacement of *A. wrangelianus*. In this model, the only options are the empty set, the community containing only *H. murinum*, and the community containing only *P. erecta*. In order for the displacement event to occur, all species in the pre-invasion community that are not in the post-invasion community must have a negative invasion growth rate (Hofbauer and Schreiber, 2022).

This clearly is not the case for the empty set as all species can invade the empty set. As previously established, *A. wrangelianus* has a positive invasion growth rate in a community containing only *H. murinum*, so we know that *H. murinum* does not competitively exclude *A.*

wrangelianus. The last candidate then is the community containing *P. erecta*. We know from figure 8 that *A. wrangelianus* has a negative invasion growth rate at the community containing only *P. erecta*. However, we also know that *H. murinum* can successfully invade and displace *P. erecta* from figure 2A. Thus, *H. murinum* has a positive invasion growth rate the community containing *P. erecta*. Thus, we can conclude that the reason *P. erecta* cannot displace *A. wrangelianus* in this situation is because it cannot displace *H. murinum*. If *H. murinum* could be successfully displaced from this community, then *P. erecta* could subsequently displace *A. wrangelianus*. However, *H. murinum*'s positive invasion growth rate at the community containing *P. erecta* prevents this possibility.

With both of these decompositions, we can conclude why *A. wrangelianus* goes extinct following the loss of *H. murinum*. In the disassembled community, *A. wrangelianus* cannot coexist with *P. erecta* since *P. erecta* is a superior competitor to *A. wrangelianus*. However, despite this, we find that *A. wrangelianus* and *H. murinum* can coexist. When *P. erecta* then invades the community with *A. wrangelianus* and *H. murinum*, it invades without displacing *A. wrangelanius*, leading to coexistence of the full community. *P. erecta* cannot displace *A. wrangelianus* in this case since this would require *H. murinum* to be unable to invade the post-invasion community. However, since *H. murinum* is a superior competitor to *P. erecta*, this is not possible, leading to coexistence of the full community. Thus, we see that persistence of *A. wrangelianus* in the full community is contingent upon the presence of *H. murinum*.

References

S. Allesina and J. M. Levine. A competitive network theory of species diversity. Proceedings of the National Academy of Sciences, 108(14):5638–5642, 2011.

R. A. Armstrong and R. McGehee. Competitive exclusion. The American Naturalist, 115(2): 151–170, 1980.

C. E. Aslan, E. S. Zavaleta, B. Tershy, and D. Croll. Mutualism disruption threatens global plant biodiversity: a systematic review. PloS one, 8(6):e66993, 2013.

M. S. Bane, M. J. Pocock, and R. James. Effects of model choice, network structure, and interaction strengths on knockout extinction models of ecological robustness. Ecology and evolution, 8(22):10794–10804, 2018.

G. Barabás, R. D'Andrea, and S. M. Stump. Chesson's coexistence theory. Ecological monographs, 88(3):277–303, 2018.

J. Bascompte and D. B. Stouffer. The assembly and disassembly of ecological networks. Philosophical Transactions of the Royal Society B: Biological Sciences, 364(1524):1781–1787, 2009.

J. F. Brodie, C. E. Aslan, H. S. Rogers, K. H. Redford, J. L. Maron, J. L. Bronstein, and C. R. Groves. Secondary extinctions of biodiversity. Trends in ecology & evolution, 29(12):664–672, 2014.

P. Chesson. Multispecies competition in variable environments. Theoretical population biology, 45(3):227–276, 1994.

A. T. Clark, L. G. Shoemaker, J.-F. Arnoldi, G. Barabás, R. Germain, O. Godoy, L. Hallett, C. Karakoç, S. Saavedra, and S. Schreiber. A practical guide to quantifying ecological coexistence. 2024.

R. K. Colwell, R. R. Dunn, and N. C. Harris. Coextinction and persistence of dependent species in a changing world. Annual Review of Ecology, Evolution, and Systematics, 43(1): 183–203, 2012.

J. A. Dunne, R. J. Williams, and N. D. Martinez. Food-web structure and network theory: the role of connectance and size. Proceedings of the National Academy of Sciences, 99(20): 12917–12922, 2002a.

J. A. Dunne, R. J. Williams, and N. D. Martinez. Network structure and biodiversity loss in food webs: robustness increases with connectance. Ecology letters, 5(4):558–567, 2002b.

J. A. Dunne, R. J. Williams, and N. D. Martinez. Network structure and robustness of marine food webs. Marine Ecology Progress Series, 273:291–302, 2004.

B. Ebenman and T. Jonsson. Using community viability analysis to identify fragile systems and keystone species. Trends in Ecology & Evolution, 20(10):568–575, 2005.

K. F. Edwards and S. J. Schreiber. Preemption of space can lead to intransitive coexistence of competitors. Oikos, 119(7):1201–1209, 2010.

S. P. Ellner, R. E. Snyder, P. B. Adler, and G. Hooker. An expanded modern coexistence theory for empirical applications. Ecology letters, 22(1):3–18, 2019.

S. P. Ellner, R. E. Snyder, P. B. Adler, and G. Hooker. Toward a "modern coexistence theory"' for the discrete and spatial. Ecological Monographs, 92(4):e1548, 2022.

G. F. Gause. The struggle for existence. 1934.

I. Geijzendorffer, W. Van der Werf, F. Bianchi, and R. Schulte. Sustained dynamic transience in a lotka–volterra competition model system for grassland species. Ecological Modelling, 222(15):2817–2824, 2011.

R. M. Germain, J. L. Williams, D. Schluter, and A. L. Angert. Moving character displacement beyond characters using contemporary coexistence theory. Trends in Ecology & Evolution, 33(2):74–84, 2018.

P. W. Glynn. Some physical and biological determinants of coral community structure in the eastern pacific. Ecological monographs, 46(4):431–456, 1976.

O. Godoy, F. Soler-Toscano, J. R. Portillo, and J. A. Langa. The assembly and dynamics of ecological communities in an ever-changing world. Ecological Monographs, 94(4):e1633, 2024.

N. A. Graham, P. Chabanet, R. D. Evans, S. Jennings, Y. Letourneur, M. Aaron MacNeil, T. R. McClanahan, M. C. Öhman, N. V. Polunin, and S. K. Wilson. Extinction vulnerability of coral reef fishes. Ecology letters, 14(4):341–348, 2011.

T. N. Grainger, A. D. Letten, B. Gilbert, and T. Fukami. Applying modern coexistence theory to priority effects. proceedings of the national academy of sciences, 116(13):6205–6210, 2019a.

T. N. Grainger, J. M. Levine, and B. Gilbert. The invasion criterion: a common currency for ecological research. Trends in ecology & evolution, 34(10):925–935, 2019b.

J. Hofbauer. A general cooperation theorem for hypercycles. Monatshefte für Mathematik, 91 (3):233–240, 1981.

J. Hofbauer. Heteroclinic cycles in ecological differential equations. Equadiff 8, pages 105–116, 1994.

J. Hofbauer and S. J. Schreiber. Permanence via invasion graphs: incorporating community assembly into modern coexistence theory. Journal of mathematical biology, 85(5):54, 2022.

J. Hofbauer and K. Sigmund. Evolutionary games and population dynamics. Cambridge university press, 1998.

H. S. Horn. The ecology of secondary succession. Annual review of ecology and systematics, pages 25–37, 1974.

J. Jackson and L. Buss. Alleopathy and spatial competition among coral reef invertebrates. Proceedings of the National Academy of Sciences, 72(12):5160–5163, 1975.

F. Jordán. Keystone species and food webs. Philosophical Transactions of the Royal Society B: Biological Sciences, 364(1524):1733–1741, 2009.

P.-J. Ke and A. D. Letten. Coexistence theory and the frequency-dependence of priority effects. Nature Ecology & Evolution, 2(11):1691–1695, 2018.

R. Kehoe, E. Frago, and D. Sanders. Cascading extinctions as a hidden driver of insect decline. Ecological Entomology, 46(4):743–756, 2021.

B. Kerr, M. A. Riley, M. W. Feldman, and B. J. Bohannan. Local dispersal promotes biodiversity in a real-life game of rock–paper–scissors. Nature, 418(6894):171–174, 2002.

A. A. Keyes, A. K. Barner, and L. E. Dee. Synthesising the relationships between food web structure and robustness. Ecology Letters, 27(10):e14533, 2024.

R. E. Langendorf, J. A. Estes, J. C. Watson, M. C. Kenner, B. B. Hatfield, M. T. Tinker, E. Waddle, M. L. DeMarche, and D. F. Doak. Dynamic and context-dependent keystone species effects in kelp forests. Proceedings of the National Academy of Sciences, 122(10): e2413360122, 2025.

M. Letnic, F. Koch, C. Gordon, M. S. Crowther, and C. R. Dickman. Keystone effects of an alien top-predator stem extinctions of native mammals. Proceedings of the Royal Society B: Biological Sciences, 276(1671):3249–3256, 2009.

J. M. Levine, J. Bascompte, P. B. Adler, and S. Allesina. Beyond pairwise mechanisms of species coexistence in complex communities. Nature, 546(7656):56–64, 2017.

J. Lubchenco. Plant species diversity in a marine intertidal community: importance of herbivore food preference and algal competitive abilities. The American Naturalist, 112(983):23–39, 1978.

R. MacArthur and R. Levins. The limiting similarity, convergence, and divergence of coexisting species. The american naturalist, 101(921):377–385, 1967.

M. Manhart and E. I. Shakhnovich. Growth tradeoffs produce complex microbial communities on a single limiting resource. Nature communications, 9(1):3214, 2018.

R. M. May and W. J. Leonard. Nonlinear aspects of competition between three species. SIAM journal on applied mathematics, 29(2):243–253, 1975.

K. McCann, A. Hastings, and G. R. Huxel. Weak trophic interactions and the balance of nature. Nature, 395(6704):794–798, 1998.

J. Memmott, N. M. Waser, and M. V. Price. Tolerance of pollination networks to species extinctions. Proceedings of the Royal Society of London. Series B: Biological Sciences, 271 (1557):2605–2611, 2004.

M. L. Moir, P. A. Vesk, K. E. Brennan, D. A. Keith, L. Hughes, and M. A. McCARTHY. Current constraints and future directions in estimating coextinction. Conservation Biology, 24(3):682–690, 2010.

S. D. Mylius and O. Diekmann. The resident strikes back: invader-induced switching of resident attractor. Journal of Theoretical Biology, 211(4):297–311, 2001.

S. D. Mylius, M. Doebeli, and O. Diekmann. Can initial invasion dynamics correctly predict phenotypic substitutions. Advances in Adaptive Dynamics, U. Dieckmann & JAJ Metz (eds.), to appear, 1998.

R. S. Ostfeld and K. LoGiudice. Community disassembly, biodiversity loss, and the erosion of an ecosystem service. Ecology, 84(6):1421–1427, 2003.

R. T. Paine. Food web complexity and species diversity. The American Naturalist, 100(910): 65–75, 1966.

R. T. Paine. A note on trophic complexity and community stability. The American Naturalist, 103(929):91–93, 1969.

R. T. Paine. Food webs: linkage, interaction strength and community infrastructure. Journal of animal ecology, 49(3):667–685, 1980.

R. T. Paine, J. Terborgh, and J. Estes. Food chain dynamics and trophic cascades in intertidal habitats. Trophic cascades: predators, prey, and the changing dynamics of nature, pages 21–35, 2010.

A. I. Pastore, G. Barabás, M. D. Bimler, M. M. Mayfield, and T. E. Miller. The evolution of niche overlap and competitive differences. Nature Ecology & Evolution, 5(3):330–337, 2021.

S. C. Pennings and R. M. Callaway. Impact of a parasitic plant on the structure and dynamics of salt marsh vegetation. Ecology, 77(5):1410–1419, 1996.

R. Ranjan, T. Koffel, and C. A. Klausmeier. The three-species problem: Incorporating competitive asymmetry and intransitivity in modern coexistence theory. Ecology Letters, 27(4): e14426, 2024.

S. J. Schreiber. On the stabilizing effect of specialist predators on founder-controlled communities. Canadian Applied Math. Quart, 6:195–206, 1998.

S. J. Schreiber. Criteria for C^r robust permanence. Journal of Differential Equations, 162(2): 400–426, 2000.

S. J. Schreiber. Persistence despite perturbations for interacting populations. Journal of Theoretical Biology, 242(4):844–852, 2006.

S. J. Schreiber. Coexistence and extinction in flow-kick systems: An invasion growth rate approach. arXiv preprint arXiv:2507.02157, 2025.

S. J. Schreiber and S. Rittenhouse. From simple rules to cycling in community assembly. Oikos, 105(2):349–358, 2004.

S. J. Schreiber, M. Yamamichi, and S. Y. Strauss. When rarity has costs: coexistence under positive frequency-dependence and environmental stochasticity. Ecology, 100(7):e02664, 2019.

L. G. Shoemaker, A. K. Barner, L. S. Bittleston, and A. I. Teufel. Quantifying the relative importance of variation in predation and the environment for species coexistence. Ecology Letters, 23(6):939–950, 2020.

H. L. Smith. Monotone dynamical systems: An introduction to the theory of competitive and cooperative systems. Number 41. American Mathematical Society, 1995.

H. L. Smith. Planar competitive and cooperative difference equations. Journal of Difference Equations and Applications, 3(5-6):335–357, 1998.

K. Soetaert, T. Petzoldt, and R. W. Setzer. Solving differential equations in r: package desolve. Journal of statistical software, 33:1–25, 2010.

C. Song and J. W. Spaak. Trophic tug-of-war: Coexistence mechanisms within and across trophic levels. Ecology Letters, 27(4):e14409, 2024.

J. W. Spaak and S. J. Schreiber. Building modern coexistence theory from the ground up: the role of community assembly. Ecology Letters, 26(11):1840–1861, 2023.

J. J. Stachowicz. Mutualism, facilitation, and the structure of ecological communities: positive interactions play a critical, but underappreciated, role in ecological communities by reducing physical or biotic stresses in existing habitats and by creating new habitats on which many species depend. Bioscience, 51(3):235–246, 2001.

J. J. Stachowicz and M. E. Hay. Mutualism and coral persistence: the role of herbivore resistance to algal chemical defense. Ecology, 80(6):2085–2101, 1999.

G. Strona and C. J. Bradshaw. Co-extinctions annihilate planetary life during extreme environmental change. Scientific reports, 8(1):16724, 2018.

Y. Tang, F. Wang, and W. Zhou. Network structure indicators predict ecological robustness in food webs. Ecological Research, 39(5):766–774, 2024.

D. Tilman. Resource competition and community structure. Number 17. Princeton university press, 1982.

M. N. Van Dyke, J. M. Levine, and N. J. Kraft. Small rainfall changes drive substantial changes in plant coexistence. Nature, 611(7936):507–511, 2022.

A. J. Vanbergen, B. A. Woodcock, M. S. Heard, and D. S. Chapman. Network size, structure and mutualism dependence affect the propensity for plant–pollinator extinction cascades. Functional ecology, 31(6):1285–1293, 2017.

J. Vandermeer. Transitive and intransitive structures in competition-based ecological communities. Ecological Complexity, 60:101103, 2024.

D. A. Vasseur and J. W. Fox. Environmental fluctuations can stabilize food web dynamics by increasing synchrony. Ecology letters, 10(11):1066–1074, 2007.

C. A. Wainright, C. C. Muhlfeld, J. J. Elser, S. L. Bourret, and S. P. Devlin. Species invasion progressively disrupts the trophic structure of native food webs. Proceedings of the National Academy of Sciences, 118(45):e2102179118, 2021.

A. D. Wallach, W. J. Ripple, and S. P. Carroll. Novel trophic cascades: apex predators enable coexistence. Trends in Ecology & Evolution, 30(3):146–153, 2015.

J. P. Wright, C. G. Jones, and A. S. Flecker. An ecosystem engineer, the beaver, increases species richness at the landscape scale. Oecologia, 132:96–101, 2002.

J. D. Yeakel, M. M. Pires, M. A. de Aguiar, J. L. O'Donnell, P. R. Guimarães Jr, D. Gravel, and T. Gross. Diverse interactions and ecosystem engineering can stabilize community assembly. Nature communications, 11(1):3307, 2020.

E. Zavaleta, J. Pasari, J. Moore, D. Hernandez, K. B. Suttle, and C. C. Wilmers. Ecosystem responses to community disassembly. Annals of the New York Academy of Sciences, 1162 (1):311–333, 2009.

L. Zhou, W. Liu, L. Bai, H. Liu, J. Wang, X. Ma, L. Huang, K. Guo, H. Yu, and J. Hu. Female's war: a story of the invasion and competitive displacement between two xylophilus group nematode species. Journal of Pest Science, 96(3):1301–1311, 2023.